Modeling Driver Response to Lead Vehicle Decelerating

Wassim G. Najm
Volpe National Transportation Systems Center

David L. Smith
National Highway Traffic Safety Administration

ABSTRACT

This paper presents a driver performance map of braking and steering in response to three driving scenarios that lead to rear-end crashes. This map encompasses low risk, conflict, near-crash, and crash imminent driving states that correspond to advisory warning, crash imminent warning, and crash mitigation functionalities for intelligent vehicle rear-end crash countermeasures. Specifically, this paper models driver response to a lead vehicle decelerating by building upon prior research that estimated the state boundaries for driver response to lead vehicle stopped or moving at slower constant speed. In addition, this paper compares braking performance to steering performance in the lead vehicle-decelerating scenario using plots of range and range-rate that roughly quantify the boundaries between the driving conflict states. Driver performance is also discussed among the three rear-end crash scenarios.

INTRODUCTION

Four driving conflict states have been identified to form the foundation of driver performance maps that consist of low risk, conflict, near-crash, and crash imminent driving states [1]. This performance mapping structure corresponds to crash countermeasures that assist drivers via advisory, crash imminent warning, automatic vehicle control, or crash injury mitigation functions. In addition, this map enables the integration of disparate databases on driver performance observed in such varied media as test tracks, simulators, naturalistic on-road experiments, and field operational tests. The development of these maps leads to the unambiguous and quantitative definition of boundaries between the four driving conflict states. These boundaries then allow researchers to perform the proper reduction of data collected during driving studies, combine and compare data files from different studies, and establish consistency in assessing the safety impact of crash avoidance systems among independent evaluations.

The feasibility of the performance mapping structure was previously investigated, where it was found that the driving state boundaries could be reliably quantified using range and range-rate metrics based on the judgments of alert and aware drivers [1]. The drivers' opinions as expressed in their braking or steering performance constituted the basis for assigning the levels of driving conflict states in different traffic scenarios. It was assumed that initial braking or steering onset indicated when drivers judge the start of the dynamic event as they followed "last-second maneuver" instructions. This approach utilized performance data gathered from test-track controlled studies in which subjects were instructed to wait to conduct a maneuver (brake or steer) at the last possible moment in order to avoid colliding with a vehicle using normal or hard intensity. Thus, drivers indicated their sense of conflict onset through last-second normal intensity maneuvers, and they showed their sense of near-crash onset through last-second hard intensity maneuvers. The onset of the crash imminent state was determined by the start of evasive maneuvers that result in a crash. Such data might be obtained from driving simulator experiments or on-road naturalistic driving studies.

Follow-on analysis of braking and steering performance in two vehicle-following scenarios, an encounter between a following vehicle and a lead vehicle stopped (LVS) or moving at lower constant speed (LVM), revealed that distinct driving state boundaries must be established for different driver responses to each dynamic scenario encountered in the driving environment [2]. The roughly quantified boundaries between the low risk and conflict driving states, and between the conflict and near-crash states, depended on the dynamic scenario when drivers responded by braking only. Drivers were generally less aggressive in the LVM scenario than in the LVS scenario. On the other hand, the steering response was independent of the two dynamic scenarios. Moreover, the roughly quantified boundaries of the driving states varied between braking and steering driver responses since drivers initiated last-second braking maneuvers at

generally longer distances than last-second steering maneuvers in order to avoid a lead vehicle ahead.

This paper presents results from a recent analysis that builds upon prior research on estimating the state boundaries for the LVS and LVM scenarios based on driver performance [2]. The results are extended to the lead vehicle decelerating (LVD) scenario so as to create comprehensive driver performance maps for rear-end crash avoidance research. Eventually, it will be necessary to establish standardized quantifications for the driving state boundaries, though this was determined to be beyond the scope of this current work. Instead, this paper focuses on using the existing driver performance databases to roughly estimate and assess the quantified boundaries in the LVD scenario based on braking and steering maneuvers. The LVD scenario preceded about 57% of the 1,806,000 police-reported rear-end crashes in the United States, which involved light vehicles (passenger vehicles, sport utility vehicles, vans, and pickup trucks) based on the 2000 *National Automotive Sampling System/General Estimates System* crash database [3]. Collectively, the LVD, LVS, and LVM scenarios accounted for about 96% of these rear-end crashes.

The analysis herein utilizes driver performance data sets collected by the GM-Ford Crash Avoidance Metrics Partnership (CAMP) from test track studies, and crash data sets obtained from the Iowa Driving Simulator (IDS) by the University of Iowa. CAMP collected data sets on driver performance from test track studies to develop a fundamental understanding of drivers' last-second braking and last-second steering performance so that drivers' perceptions could be properly identified and modeled for collision warning system crash alert timing purposes [4,5]. CAMP generated data from 4,326 last-second maneuver trials conducted in two separate studies, including 3,536 last-second braking judgment trials and 790 last-second steering judgment trials. The first study collected braking judgment data from 2,580 trials in response to the LVS and LVD scenarios [4]. The second study obtained additional data from 1,746 trials that involved last-second braking and last-second steering maneuvers in response to LVS, LVM, and LVD scenarios [5]. The IDS study investigated different alert timings for a rear-end crash warning algorithm by examining how drivers react when purposefully distracted at the moment when a lead vehicle suddenly decelerates ahead after a period of vehicle following at constant speed [6]. Our analysis used crash data from the baseline condition – without the assistance of a rear-end crash warning system.

This paper first delineates the modeling approach and data binning technique used for our analysis. After, this paper describes the boundaries between the four driving conflict states based on the initial braking response to the LVD scenario. The results are then compared to the boundaries of the LVS and LVM scenarios based on

braking response. Afterwards, this paper estimates state boundaries based on the initial steering response to the LVD scenario. This is followed by a comparison between LVD steering response and LVS and LVM steering responses. Later, this paper discusses the results from both braking and steering responses. Finally, this paper recaps overall results and recommends future research steps.

METHODOLOGY

MODELING APPROACH

First, it is important to understand the rationale behind our selection of the range and range-rate as the two metrics to characterize the vehicle-following dynamics. Figure 1 illustrates the general kinematic situation of vehicle following. Here, each vehicle has a position on the road measured by the variable x. The range is the difference between the two x's. Each vehicle is thus described by Newtonian mechanics of motion where the sum of the forces acting on the vehicle will lead to change in its motion. For example for the lead vehicle,

$$\Sigma F_L = m_L \times a_L = m_L \times d^2x_L / dt^2 \tag{1}$$

ΣF_L refers to the sum of forces acting on the lead vehicle, while m_L and a_L indicate respectively the mass and acceleration of the lead vehicle. Furthermore, we can create a simple model of vehicle dynamics by expanding the left side of Equation (**1**) as follows:

$$\Sigma F_L = T_L - B_L \tag{2}$$

T_L denotes the forward thrust exerted on the lead vehicle by the engine, and B_L refers to the net braking exerted by the driver of the lead vehicle. Note that grade and drag are neglected. Moreover, T_L and B_L are both inputs under the control of the driver. After substituting u for the input variables and rearranging, the equation of longitudinal motion thus becomes:

$$m_L \times d^2x_L / dt^2 = C_{T1} \times u_{aL} - C_{B1} \times u_{bL} \tag{3}$$

Equation (**3**) represents a linear constant-coefficient state-space system equation. u_{aL} and u_{bL} are respectively the engine and braking control inputs to the lead vehicle, while C_{T1} and C_{B1} are their corresponding coefficients. Note that we could formulate a very similar equation for the following vehicle. When we divide by the masses, and subtract, what we find is that the inter-vehicle dynamics follow the relationship:

$$d^2R/dt^2 = f(u_{aL}, u_{aF}, u_{bL}, u_{bF}) \tag{4}$$

That is, either driver may exert braking or acceleration through the input brake pedal or the accelerator pedal to affect change in the range, R. In reality, drivers could also

2

provide an input in steering, though we have neglected that to clarify the above longitudinal kinematics.

Of course, it can be recognized from Equation (**4**) that the inter-vehicle longitudinal dynamics are thus a linear
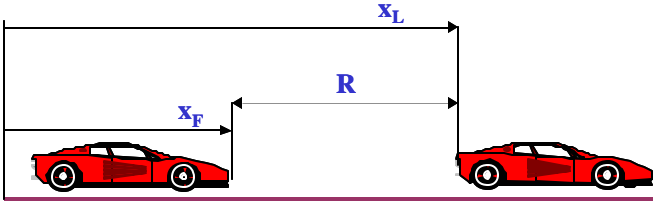

Figure 1. Kinematic Illustration of Vehicle-Following Scenarios

second-order system. Two states are thus necessary and sufficient to characterize the dynamics. The two states that would normally be chosen to model the system described by Equation (**4**) would be the range and range-rate. This is fortunate for our driver performance analysis in that these are the same two states that drivers are able to judge well. Hence, we chose to use the range/range-rate diagram to display results, which is exactly the same as a system engineer's usual state space diagram, also known as a phase diagram, for longitudinal vehicle dynamics. Our explanation of the test scenarios is that the drivers see the range decreasing and they react through their control inputs - we seek to characterize the point at which they begin to exert control input via braking or steering.

DATA BINNING TECHNIQUE

The following vehicle initially maintains constant speed and range behind the lead vehicle in the LVD scenario. At the onset of braking by the lead vehicle, the range (R) between the two vehicles starts to decrease, while the closing rate (Rdot) increases. Unlike the LVS and LVM scenarios in which Rdot remained constant, the driver of the following vehicle must initiate braking or steering in response to varying R and Rdot. The rate of change in R and Rdot depends on the deceleration level of the lead vehicle. The initial conditions of this scenario are represented by the initial vehicle speed, initial range, and lead vehicle deceleration. In the absence of a following vehicle response, the equation below characterizes the kinematics of the LVD scenario for a constant lead vehicle deceleration before the following vehicle starts braking as shown in the top part of the curve in Figure 2:

$$R = R_0 + \frac{Rdot^2}{2 \times a_L} \qquad (5)$$

Note that this equation is a solution to the purely kinematic relationships $R = \Delta x$, $v = dx/dt$, and $a = dv/dt$. It is thus a different relationship than that of Equation (**4**), which shows the relationships between the forces and the

motion. Here, we see the relationship between the motion variables due solely to lead vehicle deceleration.

Equation (**5**) thus describes a curve in R, Rdot that starts at the vertical R axis of Figure 2 (the initial platooning condition) and loops down to the left as the range decreases while the range-rate increases. If the following vehicle did not brake at all, this curve would eventually intersect the R= 0 axis, thus indicating a crash. The parameter a_L (m/s^2) denotes the deceleration of the lead vehicle, while R_0 (m) refers to the initial range prior to lead vehicle braking. Figure 2 also plots the range versus the range-rate as a result of the subsequent following vehicle braking response in the part of the curve in the figure that heads back towards the vertical axis. The following vehicle begins braking at the point where the two curves intersect and is denoted by the symbol subscript, B, on the metrics.
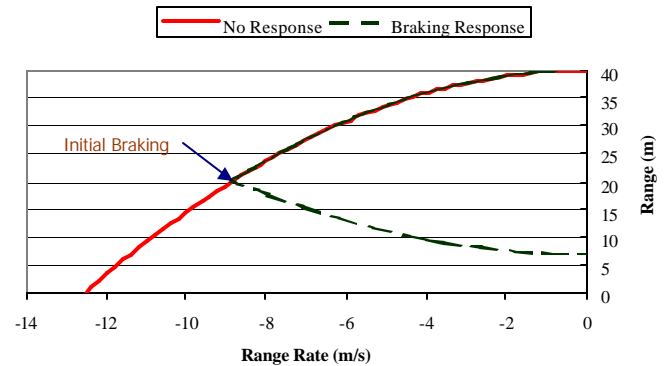

Figure 2. Trajectory of Lead Vehicle Decelerating Scenario *with* and *without* Following Vehicle Braking Response

As we began our analysis, the experimental data were separated into bins to collect similar, kinematically comparable initial conditions. Figure 3 illustrates our data binning technique for the LVD scenario by demonstrating our approach to obtain the median initial response for each bin and to approximate the best-fit line for these median values across all bins. The binning of data allows us to examine and characterize the statistical distribution (mean, median, variance, and type) of driver behavior under separate initial conditions in each driving scenario. The median statistic was used because the bin "average" or a simple fit to the cloud of data was assumed to give too much weight to the outlying range values. For example, Figure 3 shows nine vehicle trajectories observed from LVD trials, grouped three in each bin by the initial range between the two vehicles at the braking onset of the lead vehicle. Bin C represents the 30 m bin and contains all range and range-rate data pairs at the braking onset of the following vehicle for initial separation distances between 27.5 and 32.5 m. In our actual data processing, the median value was computed for each bin with at least 10 experimental data points. Finally, a best-

fit line or curve was approximated to estimate the overall response across all median values. *Microsoft Excel* software was utilized to generate the regression equations that provide rough estimates of the boundaries between the low risk and conflict driving states, and between the conflict and near-crash driving states.
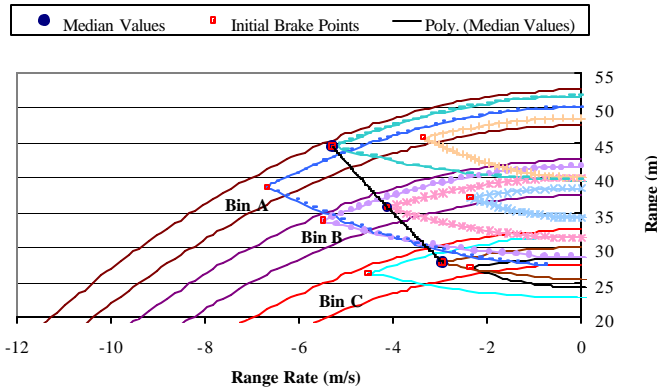

Figure 3. Binning Approach, Median Initial Response, and Best-Fit line for Vehicle Trajectories in Lead Vehicle Decelerating Scenario

ANALYSIS OF LAST-SECOND BRAKING PERFORMANCE

RESULTS OF BRAKING ANALYSIS

During CAMP's LVD braking trials, subjects followed a lead vehicle towing a 3-dimensional mock-up of the rear-end of a 1997 Mercury Sable with working brake lights at 13, 20, or 27 m/s, and were given ample time to maintain and stabilize at what they considered to be their normal following distance. Later, the lead vehicle automatically braked to a stop according to a pre-specified braking profile, resulting in constant deceleration of 0.15, 0.28, or 0.39g with the brake lights activated. The subjects were asked to wait to apply the brakes at the last possible moment in order to avoid colliding with the surrogate target, utilizing normal braking and hard braking instructions. The term "drivers" in the remainder of this paper refers to the subjects participating in these experiments.

A total of 464 normal braking data points were sorted out into bins representing various combinations of R_0, a_L, and v_{F0} rounded respectively to 5 m, 0.05g, and 2.2 m/s bins. The parameter v_{F0} (m/s) denotes the initial speed of the following vehicle prior to braking. This process resulted in 30 bins, each with at least 10 $Rdot_B$ values. The parameter $Rdot_B$ (m/s) denotes the range-rate at the onset of braking by the following vehicle. A linear regression approximation of the data using the 50th percentile value

from each bin provides the following relationship between R_B and the initial conditions:

$$R_B = -0.63 - 0.12 \times a_L + 0.04 \times v_{F0} + 0.92 \times R_0 \qquad (\textbf{6})$$

[r^2 = 1.00, F-observed= 2,641, $f_{0.01}(3,26)$= 4.64]

r^2 determines the degree of correlation between the estimated and actual R_B values. r^2 close to 1 indicates a strong relationship between the independent variables (a_L, v_{F0}, and R_0) and R_B. The regression equation is useful in predicting R_B if F-observed statistic is greater than $f_{0.01}$ (F-critical) value. The subscript 0.01 refers to the probability of erroneously concluding that there is a relationship between R_B and the independent variables [7].

Similarly, a total of 548 hard braking data points were sorted out into 34 bins with at least 10 $Rdot_B$ values each. The linear regression approximation of the hard braking data based on the bin 50th percentile values is expressed as:

$$R_B = -3.99 - 0.86 \times a_L + 0.14 \times v_{F0} + 0.80 \times R_0 \qquad (\textbf{7})$$

[r^2 = 0.98, F-observed= 578, $f_{0.01}(3,30)$= 4.51]

Equations (**6**) and (**7**) show that drivers chose R_B to brake under last-second normal and hard braking instructions based mostly on their initial range, R_0, using 50th percentile statistics. Perhaps, some drivers reacted to the brake lights of the lead vehicle instead of abiding by the last-second braking instruction. Generally, drivers follow other vehicles at a distance they feel very comfortable with based on their travel speed. Moreover, some drivers maintain the same following distance as other drivers who drive at lower speeds. When this following distance decreases due to lead vehicle braking, drivers begin to brake the moment their individual comfort level has been surpassed. To compensate for those drivers who react early to lead vehicle braking, the 85th percentile statistic was adopted for our LVD analysis instead of the median used for LVS and LVM data. The linear regression approximation of the LVD normal braking data using the 85th percentile value from each bin becomes:

$$R_B = -1.24 - 0.31 \times a_L + 0.05 \times v_{F0} + 0.86 \times R_0 \qquad (\textbf{8})$$

[r^2 = 0.99, F-observed= 1,042, $f_{0.01}(3,26)$= 4.64]

Equation (**8**) still shows that the range at the braking onset of the following vehicle is heavily associated with the range at the braking onset of the lead vehicle, given that a_L is limited to about 0.75g and v_{F0} may reach a maximum value of 36 m/s. As a result, the data were binned by R_0 without accounting for a_L and v_{F0}, yielding 14 bins with 837 data points. The following relationship between R_B and $Rdot_B$ at the braking onset of the following vehicle represents the second order polynomial best fit for the 85th percentile values from each bin:

$$R_B = 1.04 \times Rdot_B{}^2 + 1.65 \times Rdot_B + 10 \quad [r^2 = 0.94] \qquad (\mathbf{9})$$

It should be noted that R_B was set to 10 m at $Rdot_B = 0$ m/s to ensure that the onset braking range remains equal to or greater than the onset steering range for all $Rdot_B$ values as explained later in this paper. Figure 4 provides a scatter plot for all CAMP's LVD normal braking data and draws the best-fit curve for the bin 85th percentile values. About 79% of all CAMP's LVD normal braking data points fell above this curve. However, the sparse data at the higher closing rates leads us to wonder if the best-fit curve may be too high in this area. The curve fit looks good for the data above –5 m/s, but looks too high below this point.
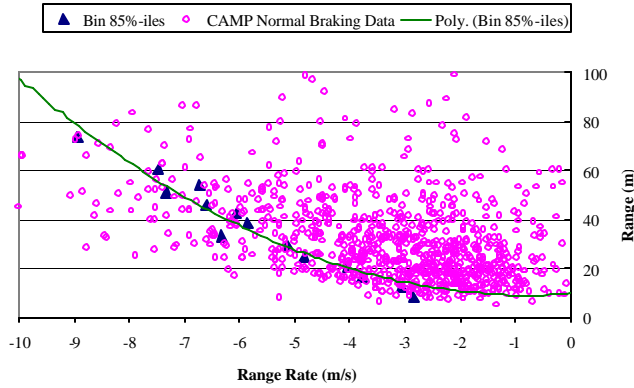
Figure 4. Normal Last-Second Braking Performance in Lead Vehicle Decelerating Scenario (85th percentile Statistics)

Following the analysis of the LVD normal braking data, 85th percentile statistics were conducted on the LVD hard braking data. The linear regression approximation of the LVD hard braking data using the 85th percentile value from each bin becomes:

$$R_B = -7.45 - 1.44 \times a_L + 0.20 \times v_{F0} + 0.7 \times R_0 \qquad (\mathbf{10})$$

$[r^2 = 0.97, \text{F-observed} = 366, f_{0.01}(3,30) = 4.51]$

The binning of the LVD hard braking data by R_0, without accounting for a_L and v_{F0}, resulted in 14 bins with 846 data points. The following relationship between R_B and $Rdot_B$ at the braking onset of the following vehicle under the hard-braking instruction represents the second order polynomial best fit for the 85th percentile values from each bin:

$$R_B = 0.2 \times Rdot_B{}^2 - 1.1 \times Rdot_B + 4.5 \quad [r^2 = 0.90] \qquad (\mathbf{11})$$

Figure 5 provides a scatter plot for all CAMP's LVD hard braking data and draws the best-fit curve for the bin 85th percentile values. About 77% of all CAMP's LVD hard braking data points fell above this curve.

An attempt was made to construct the boundary between the near-crash and crash imminent driving states using an IDS study mentioned earlier [6]. Four bins of data containing 20 trials each were available from this study, which correspond to these triads of initial conditions: ($R_0 = 27$ m, $v_{F0} = 16$ m/s, $a_L = -3.9$ m/s^2), (40 m, 16 m/s, -5.4 m/s^2), (41 m, 24 m/s, -3.9 m/s^2), and (60 m, 24 m/s, -5.4 m/s^2). A total of 64 data points involved a braking response only, which resulted in 34 crashes and 30 non-crashes. Equation (**12**) approximates the imminent crash boundary shown in Figure 6, which was devised to capture about 95% of the crash data points:

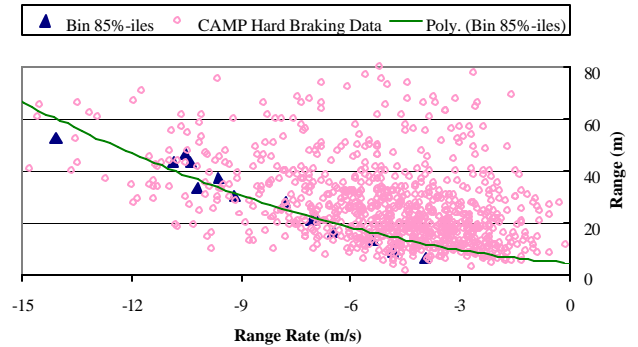$$R_B = 0.18 \times Rdot_B{}^2 \qquad (\mathbf{12})$$

Figure 5. Hard Last-Second Braking Performance in Lead Vehicle Decelerating Scenario (85th percentile Statistics)

As seen in Figure 6, 31 crash data points or about 91% of the crashes are located below the crash imminent boundary. On the other hand, 26 non-crash data points or about 87% of the non-crashes fall above this boundary.
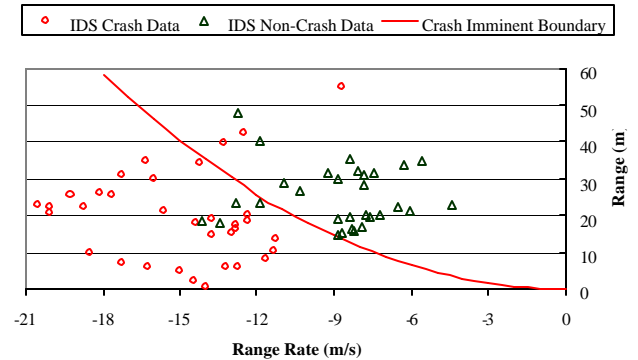

Figure 6. Braking Performance in Lead Vehicle Decelerating Scenario from IDS Driving Simulator

Figure 7 shows approximations of the four driving states based on the braking maneuver in response to the LVD scenario, using 85th percentile statistics of CAMP's last-second normal braking and hard braking trials as expressed respectively by Equations (**9**) and (**11**). In addition, the crash/non-crash boundary is drawn using Equation (**12**) based on the IDS data. The curves in Figure 7 provide rough estimates of the boundaries between the

5

low risk and conflict states, between the conflict and near-crash states, and between the near-crash and crash imminent states.

Figure 8 maps the distribution of a sample of data at the onset of braking by a following vehicle in response to a lead vehicle decelerating in traffic lane ahead, as observed in a field operational test (FOT) of an intelligent cruise control (ICC) system [8]. This distribution consists of 90 data points collected from baseline driving on state highways and arterials where vehicles were initially traveling at various speeds and ranges. Ten-Hertz video episodes as well as numerical data were collected for

Figure 7. Driving States in Lead Vehicle Decelerating Scenario Based on Braking Response (85th percentile Statistics)

this sample. The recording of video was triggered when the deceleration level from brake intervention by the host (following) vehicle or the amount of braking level required to bring the host vehicle to a headway of 0.3 second behind the lead vehicle was equal to or greater than 0.05g. The average deceleration level in each braking event by the lead vehicle varied between 0.05 and 0.15g.

As seen in Figure 8, the driver of the host vehicle applied the brakes in the low risk driving state in about 70% of the cases. Moreover, 22% and 8% of the braking response events were initiated respectively in the conflict and near-crash driving states. The analysis of average deceleration level per braking event by the host vehicle, as measured between brake pedal press and brake pedal release, showed that the overall average braking level was about 0.1g in the low risk driving state and about 0.15g in the conflict and near-crash states. As a result, the video triggering criteria in the ICC FOT captured too many episodes that were benign in terms of safety. The driving state boundaries drawn in Figure 7 could then be utilized as a filter for the lead vehicle decelerating episodes to only record safety-critical events.

Figure 8. Distribution of Braking Onset Data in Lead Vehicle Decelerating Scenario Gathered from Naturalistic Driving

COMPARISON OF BRAKING RESPONSE ACROSS SCENARIOS

Figure 9 compares the low risk/conflict boundary lines among LVS, LVM, and LVD scenarios under CAMP's last-second normal braking instruction. Similarly, Figure 10 compares the conflict/near-crash boundary lines among these scenarios under CAMP's last-second hard braking instruction. Figure 11 compares the near-crash/crash imminent boundary lines between the LVS and LVD scenarios. The phase plane (Rdot, R) analysis of initial braking data leads to consistent and orderly response patterns across many trials and conditions. As seen in Figures 9-11, parabolic lines approximate initial braking response data across scenarios and conditions. Generally, drivers are little less aggressive in the LVM scenario than in the LVS scenario based on measures of R_B and a_F. Perhaps, drivers prefer to initiate braking earlier so as to match the speed of the lead vehicle at a "comfortable" following distance. Similarly, drivers apply the brakes at longer separation distances in the LVD scenario than in the LVM and LVS scenarios especially at range-rate values below –5 m/s. It should be noted that the lead vehicle might decelerate to a stop or a lower speed in the LVD scenario. The quantified boundaries between the low risk and conflict states, between the conflict and near-crash states, and between the near-crash and crash imminent driving states thus depend on the dynamic scenario encountered in the driving environment when drivers respond by braking only.
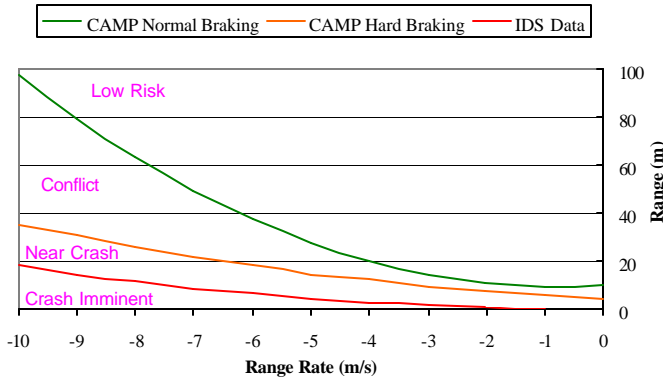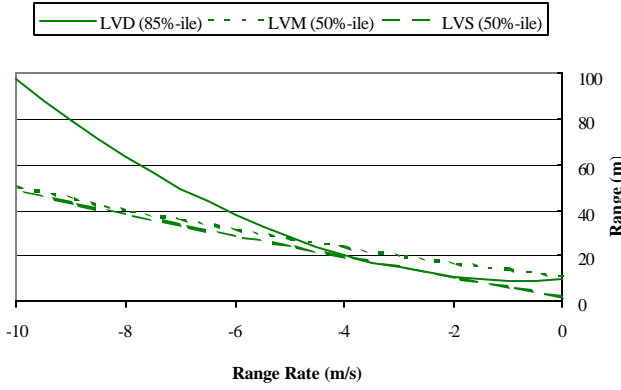
Figure 9. Comparison of Low Risk/Conflict Lines among Scenarios under Normal Braking

Figure 10. Comparison of Conflict/Near-Crash Lines among Scenarios under Hard Braking

ANALYSIS OF LAST-SECOND STEERING PERFORMANCE

RESULTS OF STEERING ANALYSIS

Similar to last-second braking instructions, drivers were asked to maintain their speed and change lanes at the last second they normally would to go around the target under "normal" steering instructions, and change lanes at the last second they possibly could to avoid colliding with the target under "hard" steering instructions. During CAMP's LVD steering trials, the following vehicle traveled at 13 and 27 m/s behind the lead vehicle. After traveling at a stabilized range for a brief duration, the lead vehicle braked at a constant deceleration of 0.15g or 0.39g with the brake lights activated. A total of 216 normal steering data points were sorted out into bins representing various combinations of R_0, a_L, and v_{F0} rounded respectively to 10 m, 0.05g, and 2.2 m/s bins. This process resulted in 14 bins, each with at least 5 combination values, which contained a total of 115 data points. A linear regression approximation of the normal steering data using the 50th percentile value from each bin provides the following relationship between the steering onset range, R_S, and the initial conditions:

$$R_S = 2 - 0.91 \times a_L + 0.11 \times v_{F0} + 0.66 \times R_0 \qquad (13)$$

$[r^2 = 0.99,\ \text{F-observed}=\ 341,\ f_{0.01}(3,10)= 6.55]$

Similarly, a total of 139 LVD hard steering data points were sorted out into bins representing various combinations of R_0, a_L, and v_{F0} rounded respectively to 10 m, 0.05g, and 2.2 m/s bins. This process resulted in 14 bins, each with at least 5 combination values, which contained a total of 105 data points. The linear regression approximation of the hard steering data based on the bin 50th percentile values is expressed as:

$$R_S = -3.3 - 2.66 \times a_L + 0.61 \times v_{F0} + 0.34 \times R_0 \qquad (14)$$

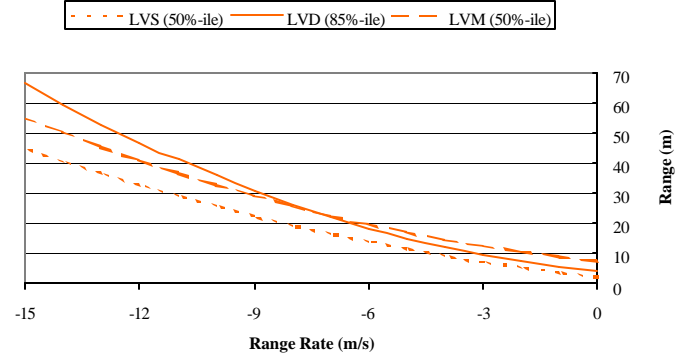$[r^2 = 0.83,\ \text{F-observed}=\ 16,\ f_{0.01}(3,10)= 6.55]$
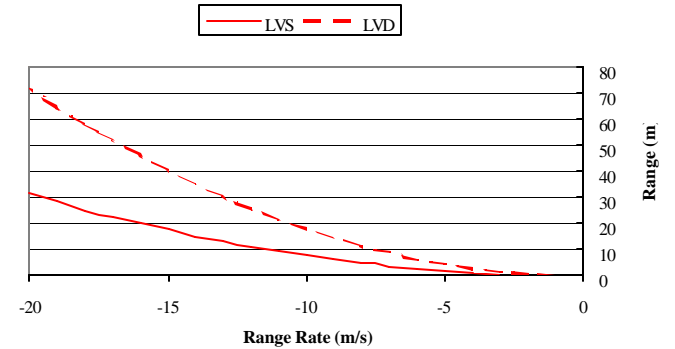

Figure 11. Comparison of Near-Crash/Crash Imminent Lines between Scenarios Based on Braking Response

To match the results against the LVD braking data, the bin 85th percentile statistics were obtained for normal and hard steering data. The linear regression approximations of the bin 85th percentile statistics in the normal and hard steering instructions are respectively:

$$R_S = 0.91 - 2.09 \times a_L + 0.09 \times v_{F0} + 0.51 \times R_0 \qquad (15)$$

$[r^2 = 0.97,\ \text{F-observed}=\ 92,\ f_{0.01}(3,10)= 6.55]$

$$R_S = -5.8 - 2.81 \times a_L + 0.51 \times v_{F0} + 0.33 \times R_0 \qquad (16)$$

$[r^2 = 0.83,\ \text{F-observed}=\ 17,\ f_{0.01}(3,10)= 6.55]$

The LVD normal steering data were binned by R_0 (5 m resolution), without accounting for a_L and v_{F0}. This process resulted in 15 bins that accounted for 195 data points. The following best-fit line equation describes the relationship between R_S and $Rdot_S$ at the steering onset of the following vehicle based on the 85th percentile values from each bin:

$$R_S = -3.66 \times Rdot_S + 3.97 \quad [r^2 = 0.88] \qquad (17)$$

Figure 12 provides a scatter plot for all CAMP's LVD normal steering data and plots the best-fit line for the bin 85th percentile values. The mapping of these data points resulted in 83% of the points falling above the best-fit line.
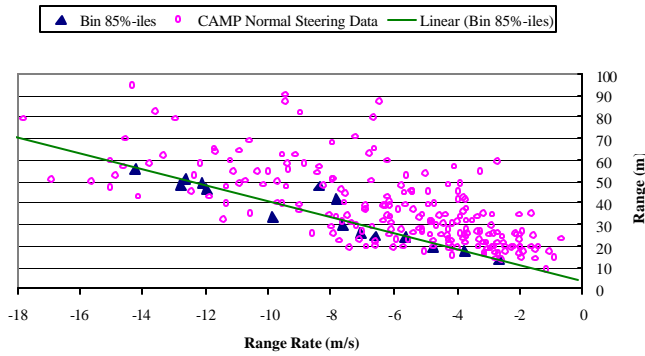
Figure 12. Normal Last-Second Steering Performance in Lead Vehicle Decelerating Scenario (85th percentile Statistics)

The LVD hard steering data were also binned by R_0 (5 m resolution), without accounting for a_L and v_{F0}. This process resulted in 11 bins that included 105 data points. The following best-fit line equation describes the relationship between R_S and $Rdot_S$ under the hard-steering instruction based on the 85th percentile values from each bin:

$$R_S = -2.52 \times Rdot_S + 2 \ [r^2 = 0.86] \tag{18}$$

The value of R_S in Equation (**18**) was set to 2 m at $Rdot_S = 0$ m/s because the best-fit line for the bin 85th percentile values yields negative values of R_S at $Rdot_S \leq 0$ m/s. Figure 13 provides a scatter plot for all CAMP's LVD hard steering data and draws the best-fit line for the bin 85th percentile values. The mapping of these data points resulted in 81% of the points falling above the line described by Equation (**18**). Figure 14 shows approximations of the driving states based on the steering maneuver in response to the LVD scenario, using 85th percentile statistics of CAMP's last-second normal steering and hard steering trials as expressed respectively by Equations (**17**) and (**18**).
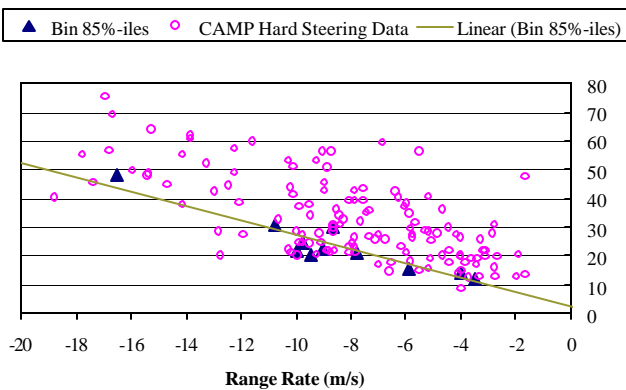

Figure 13. Hard Last-Second Steering Performance in Lead Vehicle Decelerating Scenario (85th percentile Statistics)
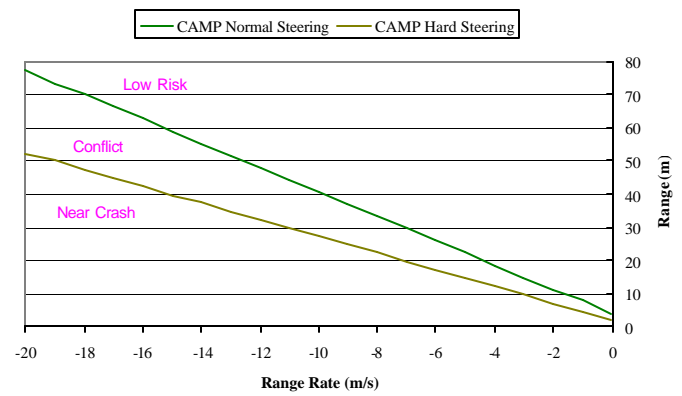

Figure 14. Driving States in Lead Vehicle Decelerating Scenario Based on Steering Response (85th percentile Statistics)

COMPARISON OF STEERING RESPONSE ACROSS SCENARIOS

Figure 15 compares the low risk/conflict boundary lines among the three scenarios under the last-second normal steering instruction, while Figure 16 compares the conflict/near-crash boundary lines among these scenarios under the last-second hard steering instruction. Similar to initial braking data, the phase plane (Rdot, R) analysis of initial steering data leads to consistent and orderly response patterns across many trials and conditions. Moreover, straight lines approximate initial steering response data across scenarios and conditions. There is a slight difference among scenarios at high closing speeds under the last-second normal steering instruction; however, the observed difference is almost negligible and thus the steering response is independent of these dynamic scenarios given the approximations made to fit CAMP's experimental data. Under the last-second hard steering instruction, the lines of the three scenarios overlap across all values of Rdot. It should be noted that the lines in Figures 15 and 16 reflect driver steering performance based on 50th percentile statistics in the LVS and LVM scenarios, and 85th percentile statistics in the LVD scenario.
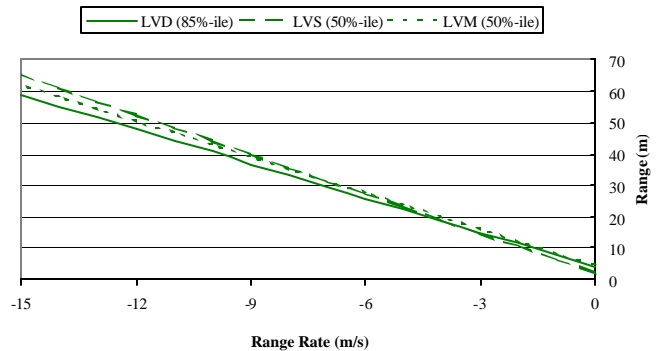

Figure 15. Comparison of Low Risk/Conflict Lines among Scenarios under Normal Steering
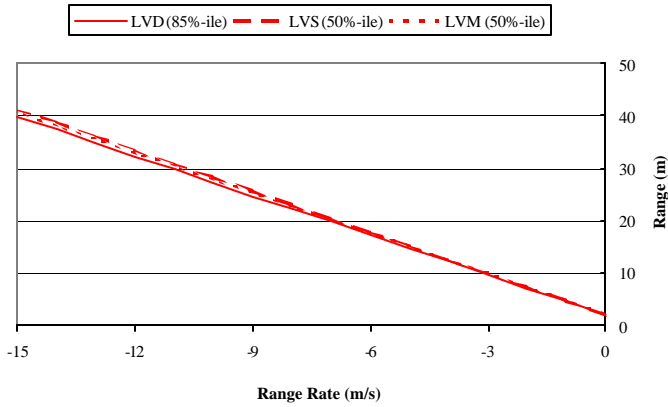
8

Figure 16. Comparison of Conflict/Near-Crash Lines among Scenarios under Hard Steering

COMPARISON BETWEEN INITIAL BRAKING AND STEERING RESPONSES

Figures 17 and 18 compare LVD braking response to LVD steering response under last-second normal and hard maneuver instructions, respectively. Generally, onset braking distances are higher than onset steering distances in the LVD scenario especially at Rdot values below –5 m/s. On the other hand, this difference appears minimal at Rdot values over –5 m/s. It should be noted that the LVD results were based on 1,683 last-second braking trials as opposed to 300 last-second steering trials. Onset braking distances were also higher than onset steering distances in the LVS and LVM scenarios. Thus, the quantified boundaries of the driving states vary between braking and steering driver responses as observed from the CAMP trials. Consequently, distinct boundaries must be established for different driver responses to each dynamic scenario encountered in the driving environment. These results point out the need to design crash warning algorithms that take into account various types of possible driver response. For instance, a rear-end crash warning algorithm based on braking response may issue alerts too early (i.e., nuisance alerts) for some drivers who plan on steering and changing lanes to avoid the vehicle in front of them. Projects are currently under way to collect on-road naturalistic data that characterize driver response to these different driving situations.
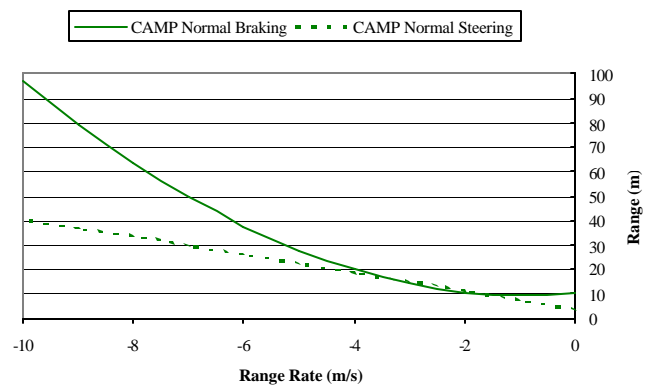

Figure 17. Comparison between Normal Braking and Normal Steering Performance in Lead Vehicle Decelerating Scenario (85th percentile Statistics)
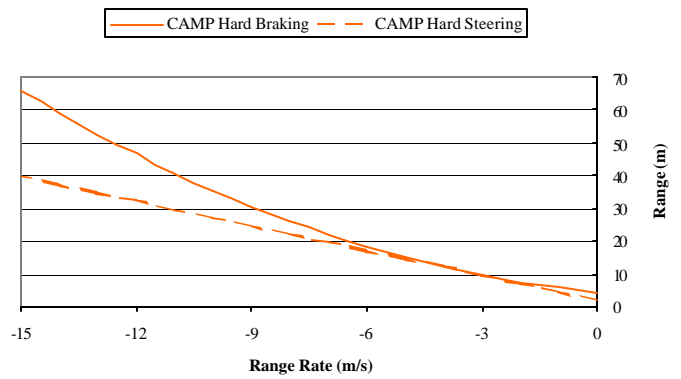

Figure 18. Comparison between Hard Braking and Hard Steering Performance in Lead Vehicle Decelerating Scenario (85th percentile Statistics)

CONCLUSION

A novel approach was described to define driving conflict states in vehicle-following scenarios based on drivers' judgment of when a driving conflict or a near-crash begins as indicated by the initiation of last-second braking or steering response with normal or hard intensity, respectively. Moreover, the start of the crash imminent state is identified from crash data in the zone where all braking actions led to a crash. Existing driver performance databases were utilized to estimate the boundaries between the driving conflict states in LVS, LVM, and LVD scenarios. Mathematical equations were derived to quantify these boundaries using 50th percentile and 85th percentile statistics, which were represented by range and range-rate data plots for various sets of initial kinematic conditions.

The median, last-second, *initial* braking points by following vehicles were observed to lie along a parabolic locus that approached the origin of the R versus Rdot plots. Note that it did not matter what the initial conditions were, the median braking responses were all initiated along this line. Of course, the subsequent trajectories would go from

9

these initial braking points back toward the origin, just as described in Figure 2. So, in a certain sense this locus could be interpreted as a measurement of the driver's *anticipation* of the median deceleration needed to safely escape the scenario under the instructed last-second conditions, for either normal or hard braking. The consistency of this notion across many drivers and many vehicle-following scenarios lends strong support to its use in defining driving conflict states.

Our analysis showed that the range and range-rate plots indicating the transitions among the various driving conflict states are distinct across the three scenarios based on last-second braking and last-second steering data. The validity of these boundaries was checked by examining onset braking data collected from naturalistic on-road studies. In summary, we now feel that the feasibility of this driver performance mapping for crash avoidance research has been demonstrated, and that we have successfully quantified most of the driving state boundaries in the vehicle-following scenarios.

Additional crash/non-crash braking performance data will be needed to identify the transition to the crash imminent state in the LVM scenario. Similarly, crash/non-crash steering performance data are required for all three scenarios. Finally, the analysis presented in this paper addresses rear-end crashes and must be extended to other crash types so as to build a comprehensive crash avoidance research database.

REFERENCES

1. Smith, D.L., Najm, W.G., and R.A. Glassco, *The Feasibility of Driver Judgment as Basis for a Crash Avoidance Database*. Paper No. 02-3695, Transportation Research Record No. 1784, Transportation Research Board 81st Annual Meeting, Washington, D.C., January 2002.
2. Smith, D.L., Najm, W.G., and A.H. Lam, *Analysis of Braking and Steering Performance in Car-Following Scenarios*. SAE 2003 World Congress, Paper No. 2003-01-0283, Detroit, MI, March 2003.
3. Najm, W.G. and J.D. Smith, *Breakdown of Light Vehicle Crashes by Pre-Crash Scenarios as a Basis for Countermeasure Development*. ASCE's 7th International Conference on Applications of Advanced Technology in Transportation, Cambridge, MA, August 2002.
4. Kiefer, R., LeBlanc, D., Palmer, M., Salinger, J., Deering, R., and M. Shulman, *Development and Validation of Functional Definitions and Evaluation Procedures for Collision Warning/Avoidance Systems*. DOT HS 808 964, NHTSA, USDOT, Washington, D.C., August 1999.
5. Kiefer, R.J., Cassar, M.T., Flannagan, C.A., LeBlanc, D.J., Palmer, M.D., Deering, R.K., and M.A. Shulman, *Forward Collision Warning Requirements Project Task 1 Final Report: Refining the CAMP Crash Alert Timing Approach by Examining 'Last-Second' Braking and Lane-Change Maneuvers Under Various Kinematic Conditions*. DOT HS 809 574, NHTSA, USDOT, Washington, D.C., January 2003.
6. Lee, J.D., McGehee, D.V., Brown, T.L., and M.L. Reyes, *Driver Distraction, Warning Algorithm Parameters, and Driver Response to Imminent Rear-End Collisions in a High-Fidelity Driving Simulator*. DOT HS 809 448, NHTSA, USDOT, Washington, D.C., March 2002.
7. Walpole, R.E., Myers, R.H, and S.L. Myers, *Probability and Statistics for Engineers and Scientists*. Sixth Edition, Prentice Hall, 1998.
8. Koziol, J., Inman, V., Carter, M., Hitz, J., Najm, W.G., Chen, S., Lam, A., Penic, M., Jensen, M., Baker, M., Robinson, M., and C. Goodspeed, *Evaluation of the Intelligent Cruise Control System, Volume I - Study Results*. DOT-VNTSC-NHTSA-98-3, DOT HS 808 969, October 1999.

DEFINITIONS, ACRONYMS, ABBREVIATIONS

a_L: Acceleration of Lead Vehicle
B_L: Lead Vehicle Braking Force
CAMP: Crash Avoidance Metrics Partnership
F_L: Force Acting on Lead Vehicle
FOT: Field Operational Test
ICC: Intelligent Cruise Control
IDS: Iowa Driving Simulator
LVD: Lead Vehicle Decelerating
LVM: Lead Vehicle Moving at Lower Constant Speed
LVS: Lead Vehicle Stopped
m_L: Lead Vehicle Mass
R: Range
R_B: Range at Onset of Braking by Following Vehicle
Rdot: Range-Rate
Rdot_B: Range-Rate at Onset of Braking by Following Vehicle
Rdot_S: Range-Rate at Onset of Steering by Following Vehicle
R_S: Range at Onset of Steering by Following Vehicle
R_0: Initial Range Prior to Lead Vehicle Braking
T_L: Forward Thrust Exerted on Lead Vehicle
u: Control Input
v_{F0}: Initial Speed of Following Vehicle Prior to Braking